



HAL
open science

Non Spurious Mixed Spectral Element Methods for Maxwell's Equations

Gary Cohen, Alexandre Sinding

► **To cite this version:**

Gary Cohen, Alexandre Sinding. Non Spurious Mixed Spectral Element Methods for Maxwell's Equations. The 9th International Conference on Mathematical and Numerical Aspects of Waves Propagation, Jun 2009, Pau, France. hal-01956669

HAL Id: hal-01956669

<https://hal.science/hal-01956669v1>

Submitted on 17 Dec 2018

HAL is a multi-disciplinary open access archive for the deposit and dissemination of scientific research documents, whether they are published or not. The documents may come from teaching and research institutions in France or abroad, or from public or private research centers.

L'archive ouverte pluridisciplinaire **HAL**, est destinée au dépôt et à la diffusion de documents scientifiques de niveau recherche, publiés ou non, émanant des établissements d'enseignement et de recherche français ou étrangers, des laboratoires publics ou privés.

Non Spurious Mixed Spectral Element Methods for Maxwell's Equations

G. Cohen¹ and A. Sinding¹

INRIA, Domaine de Voluceau, Rocquencourt - BP 105, 78153 Le Chesnay Cedex, France, email: gary.cohen@inria.fr

1 Introduction

Solving Maxwell's equations in time domain by finite element methods (FEM) is a challenging problem from two points of view: First, one must overcome the difficult problem of inverting the mass matrix (produced by FEM) at each time-step. Secondly, one must get a good approximation of the non empty kernel of the curl operator which generates spurious waves when not well approximated.

The first point is generally solved by using a mass-lumping technique, not obvious for triangular or tetrahedral meshes [10,11] but easier and more efficient for quadrangular and hexahedral meshes. These last approaches are called spectral element methods and are particularly efficient in terms of storage and computational time in their mixed formulations described in [4,6,8].

The second point was partially overcome until now. A simple way to solve this problem is to use the first family of edge elements described in [14] which ensure a good approximation of the curl's kernel. Unfortunately, such elements provide mass-lumping only on orthogonal meshes [7]. For discontinuous Galerkin methods (DGM), spurious modes become evanescent by using a dissipative jump term as shown in [5,12,13]. Another kind of jump, based on the normal component of a $H(\text{curl})$ field was used in [5] for the second family of edge elements [15]. Unfortunately, although efficient for convex domains, this term does not provide a correct model for singularities produced by reentrant corners, as we show in this paper. For continuous elements, the problem was solved by adding a divergence penalty term, which leads to a substantial additional cost and demanded a lot of work for modeling reentrant corners [1,3,9].

In this paper, we describe a new continuous approximation of Maxwell's equations well-suited to mass-lumping and which ensures low-storage. Then, we introduce a dissipative jump derived from DGM to get rid of spurious waves for both edge and continuous elements. This new approach leads to efficient spectral elements for Maxwell's equations which are cheaper than

DGM. On the other hand, this approach provides a good approximation of singularities generated by reentrant corners.

2 The Continuous Model

We want to solve Maxwell's equations in inhomogenous anisotropic lossy medium. This model reads

Find (\mathbf{E}, \mathbf{H}) : $\Omega \times]0, T[\rightarrow \mathbb{R}^3$ such that

$$\underline{\underline{\varepsilon}} \frac{\partial \mathbf{E}}{\partial t} - \nabla \times \mathbf{H} + \underline{\underline{\sigma}} \mathbf{E} = -\mathbf{J}, \quad (1)$$

$$\underline{\underline{\mu}} \frac{\partial \mathbf{H}}{\partial t} + \nabla \times \mathbf{E} = 0, \quad (2)$$

where $\Omega \subset \mathbb{R}^3$, \mathbf{J} is a given function of time and space. $\underline{\underline{\varepsilon}}$, $\underline{\underline{\sigma}}$ and $\underline{\underline{\mu}}$ are the tensors of permittivity, conductivity and permeability which read εI_3 , σI_3 and μI_3 , where I_3 is the identity matrix, in the isotropic case.

To these equations, we add homogeneous initial conditions on (\mathbf{E}, \mathbf{H}) and the perfectly conducting condition $\mathbf{E} \times \mathbf{n} = 0$ on $\partial\Omega$.

The variational formulation of (1)-(2) can be written as

Find $\mathbf{E} \in L^2(0, T; H_0(\text{curl}, \Omega))$ and $\mathbf{H} \in L^2(0, T; [L^2(\Omega)]^3)$ such that

$$\begin{aligned} \frac{d}{dt} \int_{\Omega} \underline{\underline{\varepsilon}} \mathbf{E} \cdot \boldsymbol{\varphi} \, d\mathbf{x} - \int_{\Omega} \mathbf{H} \cdot \nabla \times \boldsymbol{\varphi} \, d\mathbf{x} \\ + \int_{\Omega} \underline{\underline{\sigma}} \mathbf{E} \cdot \boldsymbol{\varphi} \, d\mathbf{x} = - \int_{\Omega} \mathbf{J} \cdot \boldsymbol{\varphi} \, d\mathbf{x}, \quad (3) \\ \forall \boldsymbol{\varphi} \in H_0(\text{curl}, \Omega), \end{aligned}$$

$$\begin{aligned} \frac{d}{dt} \int_{\Omega} \underline{\underline{\mu}} \mathbf{H} \cdot \boldsymbol{\psi} \, d\mathbf{x} + \int_{\Omega} \nabla \times \mathbf{E} \cdot \boldsymbol{\psi} \, d\mathbf{x} = 0, \quad (4) \\ \forall \boldsymbol{\psi} \in [L^2(\Omega)]^3, \end{aligned}$$

We recall the definition of $H_0(\text{curl}, \Omega)$:

$$\begin{aligned} H_0(\text{curl}, \Omega) = \left\{ \boldsymbol{\varphi} \text{ such that } \boldsymbol{\varphi} \in [L^2(\Omega)]^3, \right. \\ \left. \nabla \times \boldsymbol{\varphi} \in [L^2(\Omega)]^3, \boldsymbol{\varphi} \times \mathbf{n} = 0 \right\} \end{aligned}$$

where \mathbf{n} is the outward unit normal of $\partial\Omega$.

Both approximations by edge or continuous elements can be derived from (3)-(4) but not discontinuous Galerkin methods.

The continuous model being defined, we can now describe the different kinds of approximations treated in this paper.

3 A General Framework for Spectral Elements

A first step for constructing mixed spectral element approximations is to define the interpolation points and functions on the unit cube \widehat{K} as follows:

Let $1 \leq i \leq r+1$, $\widehat{\varphi}_i(\widehat{x})$ a Lagrange interpolation polynomial of order r and $\{\widehat{\xi}_\ell\}_{\ell=1}^{r+1}$ the Gauss-Lobatto quadrature points on interval $[0, 1]$. These points are the interpolation points for $\widehat{\varphi}_i$, i.e. $\widehat{\varphi}_i(\widehat{\xi}_\ell) = \delta_{i\ell}$, where $\delta_{i\ell}$ is the Kronecker symbol.

Now, we define the interpolation functions on \widehat{K} as products of the above defined interpolation functions. The corresponding interpolation points are the tensor products of the 1D Gauss-Lobatto points, namely $\widehat{\xi}_{\ell,m,n} = (\widehat{\xi}_\ell, \widehat{\xi}_m, \widehat{\xi}_n)$.

So, we get $\widehat{\varphi}_{i,j,k}(\widehat{\xi}_{\ell,m,n}) = \widehat{\varphi}_i(\widehat{\xi}_\ell) \widehat{\varphi}_j(\widehat{\xi}_m) \widehat{\varphi}_k(\widehat{\xi}_n) = \delta_{i\ell} \delta_{jm} \delta_{kn}$. Of course, $\widehat{\varphi}_{i,j,k} \in Q_r$, where Q_r is the polynomial space defined as

$$Q_r = \left\{ \sum_{i=0}^r \sum_{j=0}^r \sum_{k=0}^r a_{i,j,k} x_1^i x_2^j x_3^k, a_{i,j,k} \in \mathbb{R} \right\}$$

Now, at each point $\widehat{\xi}_{i,j,k}$, we have three basis functions $\{\widehat{\varphi}_{i,j,k}^s\}_{s=1}^3$ such that $\widehat{\varphi}_{i,j,k}^s = \widehat{\varphi}_{i,j,k} \mathbf{e}_s$, where \mathbf{e}_s is a unit basis vector of \mathbb{R}^3 .

Let \mathbf{F}_p the transform such that $\mathbf{F}_p(\widehat{K}) = K_p$, where K_p is an hexahedron of a mesh \mathcal{M} . In a second step, except for continuous elements, we define the basis functions on K_p as follows:

$$\varphi_{p,i,j,k}^s \circ \mathbf{F}_p = D\mathbf{F}_p^{*-1} \widehat{\varphi}_{i,j,k}^s, \quad (5)$$

where $D\mathbf{F}_p^{*-1}$ is the transpose inverse of the Jacobian matrix of \mathbf{F}_p .

$D\mathbf{F}_p^{*-1}$ is the $H(\text{curl})$ -conforming mapping, i.e. this mapping keeps the $H(\text{curl})$ character of edge elements. Although useful for edge elements only, this definition will be used for all kinds of mixed spectral approximations for the following reason: for two basis functions defined as in (5), we have

$$\begin{aligned} & \int_{K_p} \nabla \times \varphi_{p,i,j,k}^s \cdot \varphi_{p,i',j',k'}^{s'} \, d\mathbf{x} \\ &= \text{sgn}(J_p) \int_{\widehat{K}} \widehat{\nabla} \times \widehat{\varphi}_{i,j,k}^s \cdot \widehat{\varphi}_{i',j',k'}^{s'} \, d\widehat{\mathbf{x}}, \end{aligned} \quad (6)$$

where $J_p = \det(D\mathbf{F}_p)$ is the Jacobian of $D\mathbf{F}_p$ and $\widehat{\nabla}$ is the gradient with respect to the $\widehat{\mathbf{x}}$ coordinates.

In other words, the the knowledge of the stiffness integrals of the basis functions on the unit cube and the signe of the Jacobian on K_p enable the knowledge of the stiffness integrals all over the mesh, which induces a huge gain of storage.

With these definitions and by computing all the integrals by the mean of Gauss-Lobatto quadrature rules, we get block-diagonal mass matrices and very sparse stiffness matrices which provide a low-storage and fast algorithm, as described in details in [4].

These definitions can be used for Discontinuous Galerkin Methods or edge elements [3]. The only difference will lean on the continuity properties of the elements.

4 Spectral Continuous Elements

4.1 Classical Approximation

Continuous finite elements for Maxwell's equations were first introduced on the second-order (curl-curl) equation. This approximation generates, of course, spurious waves due to the bad approximation of the divergence of the electric field. The idea to get rid of these waves is based on the well-known relation

$$\nabla \times (\nabla \mathbf{E}) = \nabla(\nabla \cdot \mathbf{E}) - \Delta \mathbf{E}. \quad (7)$$

In the vacuum or in the air (i.e. $\underline{\underline{\varepsilon}} = \varepsilon I_3$, $\underline{\underline{\mu}} = \mu I_3$ and $\underline{\underline{\sigma}} = 0$), we have $\nabla \times (\nabla \mathbf{E}) = -\Delta \mathbf{E}$ since $\nabla \cdot \mathbf{E} = 0$. So, in order to get rid of the spurious waves, one adds a penalty term in $\nabla(\nabla \cdot \mathbf{E})$. The discrete formulation using the following subspace of $H(\text{curl})$

$$\begin{aligned} \mathbf{U}_h^r &= \{\mathbf{v}_h \in [H_0^1(\Omega)]^3 \text{ such that} \\ & \forall K_j \in \mathcal{M}, \mathbf{v}_h|_{K_j} \circ \mathbf{F}_j \in (Q_r)^3\}. \end{aligned} \quad (8)$$

reads

$$\begin{aligned} & \frac{d^2}{dt^2} \int_{\Omega} \varepsilon \mathbf{E}_h \cdot \boldsymbol{\varphi}_h \, d\mathbf{x} - \int_{\Omega} \frac{1}{\mu} \nabla \times \mathbf{E}_h \cdot \nabla \times \boldsymbol{\varphi}_h \, d\mathbf{x} \\ & - \rho \int_{\Omega} \nabla \cdot \mathbf{E}_h \nabla \cdot \boldsymbol{\varphi}_h \, d\mathbf{x} = - \int_{\Omega} \mathbf{J} \cdot \boldsymbol{\varphi}_h \, d\mathbf{x}, \\ & \forall \boldsymbol{\varphi}_h \in \mathbf{U}_h^r, \end{aligned} \quad (9)$$

where $\rho \in \mathbb{R}^{+*}$.

As we said in our introduction, this approach presents a double drawback: the penalty term is expensive and we still get spurious modes for reentrant corners. For these reasons, we construct a new continuous element approximation in the next section.

4.2 Mixed Spectral Continuous Elements

The idea of our approximation is to take $\mathbf{E} \in \mathbf{U}_h^r$ and $\mathbf{H} \in \mathbf{W}_h^r$ and to derive the approximate formulation from (3)-(4). Moreover, as in the two previous approximations, we add a jump term to the second equation which is written in a discontinuous space. We get

Find $\mathbf{E}_h \in L^2(0, T; \mathbf{U}_h^r)$ and $\mathbf{H}_h \in L^2(0, T; \mathbf{W}_h^r)$ such that

$$\begin{aligned} & \frac{d}{dt} \int_{\Omega} \underline{\underline{\mathbf{E}}}_h \cdot \boldsymbol{\varphi}_h \, d\mathbf{x} - \int_{\Omega} \mathbf{H}_h \cdot \nabla \times \boldsymbol{\varphi}_h \, d\mathbf{x} \\ & + \int_{\Omega} \underline{\underline{\boldsymbol{\sigma}}}_h \cdot \boldsymbol{\varphi}_h \, d\mathbf{x} = - \int_{\Omega} \mathbf{J} \cdot \boldsymbol{\varphi}_h \, d\mathbf{x}, \end{aligned} \quad (10)$$

$\forall \boldsymbol{\varphi}_h \in \mathbf{U}_h^r$,

$$\begin{aligned} & \sum_{K_j \in \mathcal{M}} \left\{ \frac{d}{dt} \int_{K_j} \underline{\underline{\boldsymbol{\mu}}}_h \cdot \boldsymbol{\psi}_h \, d\mathbf{x} \right. \\ & + \int_{K_j} \nabla \times \mathbf{E}_h \cdot \boldsymbol{\psi}_h \, d\mathbf{x} \\ & \left. + \delta'' \int_{\partial K_j} [\mathbf{n} \times \mathbf{H}_h]_{\partial K_j}^{K_j} \cdot (\mathbf{n} \times \boldsymbol{\psi}_h) \, ds \right\} = 0, \\ & \forall \boldsymbol{\psi}_h \in \mathbf{W}_h^r. \end{aligned} \quad (11)$$

where $\delta'' \in \mathbb{R}^{+*}$.

One can easily derive the energy identity

$$\frac{d\mathcal{E}}{dt}(t) = - \sum_{K_i \cap K_j} \delta'' \| [\mathbf{H} \times \mathbf{n}]_{K_i \cap K_j} \|_{L^2}^2,$$

which shows that our penalty term is dissipative.

Now, an important algorithmic issue must be considered for this method. Actually, we don't have the good property given in (6) since

$$\begin{aligned} & \int_{K_j} \nabla \times \mathbf{E}_h \cdot \boldsymbol{\psi}_h \, d\mathbf{x} \\ & = \int_{\widehat{K}} |J_j| (\nabla \times \mathbf{E}_h) \circ \mathbf{F}_j \cdot \boldsymbol{\psi}_h \circ \mathbf{F}_j \, d\widehat{\mathbf{x}} \\ & = \int_{\widehat{K}} |J_j| (DF_j^{*-1} \widehat{\nabla}) \times \widehat{\mathbf{E}}_h \cdot DF_j^{*-1} \widehat{\boldsymbol{\psi}}_h \, d\widehat{\mathbf{x}}. \end{aligned} \quad (12)$$

(12) shows that, because of the definition of \mathbf{U}_h^r , the local character of the stiffness integral is lost. That should imply of important stiffness matrix. For this reason, we have to transform the curl term in (12) as follows

$$\begin{aligned} & (DF_j^{*-1} \widehat{\nabla}) \times \widehat{\mathbf{E}}_h \\ & = (DF_j^{*-1} \widehat{\nabla}) \times (DF_j^{*-1} DF_j^* \widehat{\mathbf{E}}_h) \\ & = \frac{DF_j}{J_j} \widehat{\nabla} \times (DF_j^* \widehat{\mathbf{E}}_h) \end{aligned} \quad (13)$$

From (13), we get

$$\begin{aligned} & \int_{K_j} \nabla \times \mathbf{E}_h \cdot \boldsymbol{\psi}_h \, d\mathbf{x} \\ & = \text{sgn}(J_j) \int_{\widehat{K}} \widehat{\nabla} \times (DF_j^* \widehat{\mathbf{E}}_h) \cdot \widehat{\boldsymbol{\psi}}_h \, d\widehat{\mathbf{x}}. \end{aligned} \quad (14)$$

(14) can be decomposed into

$$\int_{\widehat{K}} \widehat{\mathbf{v}}_h \cdot \widehat{\boldsymbol{\varphi}}_h \, d\widehat{\mathbf{x}} = \int_{\widehat{K}} (DF_j^* \widehat{\mathbf{E}}_h) \cdot \widehat{\boldsymbol{\varphi}}_h \, d\widehat{\mathbf{x}}, \quad (15)$$

$\widehat{\mathbf{v}}_h \in \mathbf{W}_h^r, \widehat{\boldsymbol{\varphi}}_h \in \mathbf{W}_h^r,$

$$\begin{aligned} & \int_{K_j} \nabla \times \mathbf{E}_h \cdot \boldsymbol{\psi}_h \, d\mathbf{x} \\ & = \text{sgn}(J_j) \int_{\widehat{K}} \widehat{\nabla} \times \widehat{\mathbf{v}}_h \cdot \widehat{\boldsymbol{\psi}}_h \, d\widehat{\mathbf{x}}. \end{aligned} \quad (16)$$

In terms of matrices, (15) leads to a simple product by a block mass matrix M_h and (16) a locally defined stiffness matrix similar to those used in the two previous methods.

The stiffness integral of (10) can be treated in the same manner:

$$\begin{aligned} & \int_{\Omega} \mathbf{H}_h \cdot \nabla \times \boldsymbol{\varphi}_h \, d\mathbf{x} \\ & = \sum_{K_j \in \mathcal{M}} \int_{K_j} \mathbf{H}_h \cdot \nabla \times \boldsymbol{\varphi}_h \, d\mathbf{x} \\ & = \sum_{K_j \in \mathcal{M}} \int_{\widehat{K}} |J_j| \mathbf{H}_h \circ \mathbf{F}_j \cdot (\nabla \times \boldsymbol{\varphi}_h) \circ \mathbf{F}_j \, d\widehat{\mathbf{x}} \\ & = \sum_{K_j \in \mathcal{M}} \text{sgn}(J_j) \int_{\widehat{K}} \widehat{\mathbf{H}}_h \cdot \widehat{\nabla} \times (DF_j^* \widehat{\boldsymbol{\varphi}}_h) \, d\widehat{\mathbf{x}} \end{aligned} \quad (17)$$

(14) and (17) show that the matrices derived from these integrals are transposed one to the other.

Now, by taking basis functions as defined in section 3 and integrating by using a Gauss-Lobatto rule, we get the following discrete problem:

$$D_h E - M_h^* R_h^* H + \Sigma_h E + \widetilde{D}_h J = 0, \quad (18)$$

$$B_h H - R_h M_h E + \delta'' S_h H = 0, \quad (19)$$

where E and H are the vectors of the degrees of freedoms for the approximate fields, and

- D_h, \widetilde{D}_h and Σ_h are diagonal matrices,
- B_h is a 3×3 symmetric block-diagonal matrix,
- M_h is a mass matrix derived from the Jacobian matrices,
- R_h is a sparse stiffness matrix which need a storage on the unit cube only (when computed element by element),
- S_h is a block-diagonal matrix.

After a leapfrog discretization in time, (18)-(19) is actually solved as follows

$$\begin{aligned}
 W^{n+\frac{1}{2}} &= R_h^* H^{n+\frac{1}{2}}, \\
 D_h \frac{E^{n+1} - E^n}{\Delta t} - M_h^* W^{n+\frac{1}{2}} \\
 + \Sigma_h \frac{E^{n+1} + E^n}{2} + \tilde{D}_h J^{n+\frac{1}{2}} &= 0, \\
 V^n &= M_h E^n \\
 B_h \frac{H^{n+\frac{1}{2}} - H^{n-\frac{1}{2}}}{\Delta t} - R_h V^n \\
 + \delta'' S_h \frac{H^{n+\frac{1}{2}} + H^{n-\frac{1}{2}}}{2} &= 0.
 \end{aligned} \tag{20}$$

where V and W are auxiliary variable.

(20)-(20) provide a low storage and fast algorithm.

The approximation being defined, we must now study its properties.

4.3 Eigenvalue Analysis

In order to test the efficiency of the jump term to get rid of the spurious modes, we compute the eigenmodes of the time-harmonic problem. in Fig. , we show that all the spurious modes are suppressed by adding the jump term. In fact, the spurious modes are shifted to the complex plane with the same sign of the imaginary part, which produces evanescent waves. This term also works for reentrant corners.

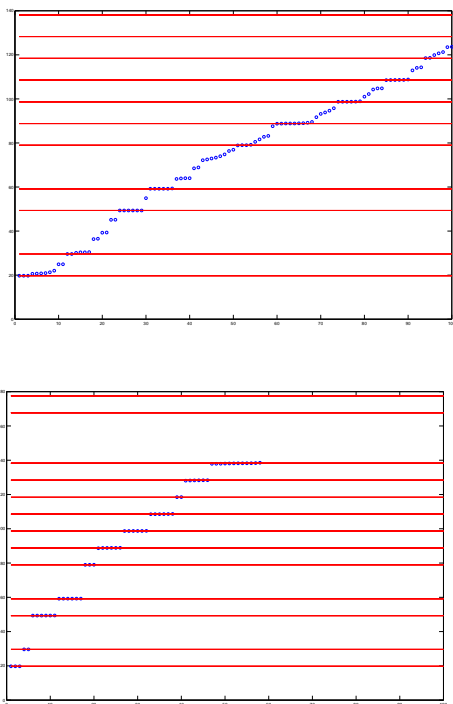


Fig. 1. Eigenmodes without dissipation (above) and with dissipation (below)

References

1. F. ASSOUS, P. CIARLET JR., J. SEGRÉ, *Numerical solution to the time-dependent Maxwell equations in axisymmetric singular domains: the singular complement method*, J. Comput. Phys. **191** (1), pp. 147–176, 2003.
2. N. CASTEL, G. COHEN, M. DURUFLÉ, *Application of Discontinuous Galerkin Methods on Hexahedral Elements for the Aeroacoustic Equation*, J. of Comp. Acous., **12** (2), pp. 175–196, 2009.
3. P. CIARLET JR., *Augmented formulations for solving Maxwell equations*, Comp. Meth. in Appl. Mech. Engrg. **194** (2-5), pp. 559–586. 2005.
4. G. COHEN, *Higher Order Numerical Methods for Transient Wave Equations*, Scientific Computation, Springer-Verlag, 2001.
5. G. COHEN, M. DURUFLÉ, *Non spurious spectral like element methods for Maxwell's equations*, Journal of Computational Mathematics, **25** (3), pp. 282–304, 2007.
6. G. COHEN AND X. FERRIERES AND S. PERNET, *A spatial high-order hexahedral discontinuous Galerkin method to solve Maxwell's equations in time domain*, J. Comput. Phys., **217**, pp. 340–363, 2006.
7. G. COHEN, P. MONK, *Gauss point mass lumping schemes for Maxwell's equations*, NMPDE Journal **14** (1), pp. 63-88, 1998.
8. G. COHEN, P. MONK, *Mur-Nédélec finite element schemes for Maxwell's equations*, Comp. Meth. in Appl. Mech. Eng., **169** (3-4), pp. 197–217, 1999.
9. M. COSTABEL, M. DAUGE, *Weighted regularization of Maxwell equation in polyhedral domains*, Numerische Mathematik, **93**, pp. 239–277, 2002.
10. A. ELMKIES, P. JOLY, *Éléments finis d'arête et condensation de masse pour les équations de Maxwell : le cas 2D*, C.R.A.S., Math., **324**, série I, pp. 1287-1293, 1997.
11. A. ELMKIES, P. JOLY, *Éléments finis d'arête et condensation de masse pour les équations de Maxwell : le cas de la dimension 3*, C.R.A.S., Math., **325**, série I, pp. 1217-1222, 1997.
12. J. S. HESTHAVEN, T. WARBURTON, *High-Order Nodal Methods on Unstructured Grids. I. Time-Domain Solution of Maxwell's Equations*, J. Comput. Phys. 181(1), pp. 186-221 (2002)
13. J. S. HESTHAVEN, T. WARBURTON, *Nodal Discontinuous Galerkin Methods Algorithms, Analysis, and Applications*, Texts in Applied Mathematics , Vol. 54, Springer-Verlag, 2008.
14. J.-C. NÉDÉLEC, *Mixed finite elements in \mathbb{R}^3* , Numer.Math., **35** (3), pp. 315-341, 1980.
15. J.-C. NÉDÉLEC, *A new family of mixed finite elements in \mathbb{R}^3* , Numer.Math., **50** (1), pp. 57-81, 1986.